



^3He - α Elastic Scattering Phase Shifts in Various Channels Using Phase Function Method with Morse Potential

Anil Khachi¹  Lalit Kumar²  and O.S.K.S. Sastri³ 

Department of Physics and Astronomical Sciences Central University of Himachal Pradesh, Dharamshala, 176216
Himachal Pradesh, Bharat (India)

*anilkhachi1990@gmail.com (Corresponding Author)

ARTICLE INFORMATION

Received: January 27, 2022
Accepted: May 14, 2022
Published Online: June 20, 2022

Keywords:

^3He - α scattering, Phase Function Method (PFM), Morse potential, cross section

ABSTRACT

Background: Typically ^3He - α reaction has been modeled using Gaussian and Hulthen potentials without incorporating the non-local spin-orbit interaction.

Purpose: To obtain the scattering phase shifts (SPS) for α - ^3He radiative capture reaction for partial waves with total angular momentum $J = 1/2, 3/2, 5/2, 7/2$ having negative parities and $J = 1/2$ with positive parity, using Morse potential as the model of interaction along with the associated spin-orbit term.

Methods: Phase function method is employed for determining phase shifts in an iterative fashion, by making changes to model parameters, to ensure minimisation of mean absolute percentage error (MAPE) w.r.t. the experimental SPS.

Results: SPS have been obtained for $1/2^+, 1/2^-, 3/2^-, 5/2^-$ and $7/2^-$ with MAPE values of 3.2, 1.0, 0.8, 17.6 and 6.5 respectively. The corresponding interaction potentials and partial cross-sections have been plotted. The resonance frequencies for the $5/2^-$ and $7/2^-$ scattering states are closely matching with experimental ones.

Conclusions: The interaction potentials for different ℓ -channels of ^7Be have been constructed by considering Morse potential and spin-orbit terms by considering experimental scattering phase shifts for ^3He - α reaction.

DOI: [10.15415/jnp.2022.92024](https://doi.org/10.15415/jnp.2022.92024)

1. Introduction

The $^3\text{He}(\alpha, \gamma)^7\text{Be}$ and $^3\text{He}(^3\text{He}, 2p)^4\text{He}$ are competing reactions in the proton-proton (p-p) chain of solar hydrogen burning and consequently determines the production of ^7Be and ^8B neutrinos in the pp-II and pp-III branches [1]. $^3\text{He}(\alpha, \gamma)^7\text{Be}$ Radiative capture reaction has been explored by various researchers [2, 9] both experimentally and theoretically and has been an interesting problem since 1960 [10]. Low energy light element scattering are interesting as well as important astrophysical processes. The reaction is important because of its importance in solar neutrino physics and nucleosynthesis [1, 3] during the beginning of time.

In $^3\text{He}(\alpha, \gamma)^7\text{Be}$ scattering astrophysical process, two protons interact to form ^2H and then protons interact with ^2H resulting in ^3He . Two ^3He nuclei come together to form ^4He which in turn mixes with another ^3He to produce ^7Be (a cluster of α and ^3He). These ^7Be nuclei interestingly produce ^7Li through e^- capture reaction. Finally, ^7Li captures a proton to form stable ^4He nuclei i.e. the production of primordial nucleosynthesis of ^7Li depends on the rate of $^4\text{He}(\alpha, \gamma)^7\text{Be}$

reaction. Although cross-sections can be directly measured at 100-500 keV energies, which is an important range for understanding the reactions during Big-Bang, they are not readily available at energies of the order of 20 KeV which are relevant in reactions happening in Sun [11]. This is because, lower energies are not currently accessible in laboratories due to Coulombic barrier that results in exponential suppression, thus not allowing measurement of cross-section for the reaction. Hence, α - ^3He reaction happening inside the sun is an interesting astrophysical problem to be studied at low energies. Also $^3\text{He}(\alpha, \gamma)^7\text{Be}(e^-, \nu)^7\text{Li}$ chain reaction is main reaction leading for ^7Li production during big bang nucleosynthesis (BBN) [2]. $^3\text{He}(\alpha, \gamma)^7\text{Be}$ reaction is having low ground state binding energy of -1.586 MeV [12], which is less than proton separation energy in ^3He of 5.5 MeV and thus is also important problem in halo effective field theory (hEFT) [13]. Microscopic models [14, 15] have been used to obtain cross-section data at lower energies through extrapolation. We have taken this particular reaction for its astrophysical importance and studied the interaction potential using Morse function. The scattering phase shifts

(SPS) have been obtained using phase function method (PFM). The model parameters are obtained by minimising the mean absolute percentage error between the calculated and experimental phase shifts data. Phase shift plays an integral role in scattering cross-section calculations which are in turn needed for astrophysical S-factor calculations. The phase shift is a signature of the interaction potential, i.e. carries the information about the interaction with it. Various methods are there in the literature for phase shift calculations, like S-matrix method [16], Jost function method [17], which utilise wave function information obtained from solving the time independent Schrodinger equation. On the other hand, *ab initio* approach [6] utilises realistic inter-nucleon interaction like renormalized chiral nucleon-nucleon interaction and is able to reproduce experimental phase shifts without any need for adjustment of parameters. Recently, *ab initio* no-core shell model with continuum (NCSMC) [6] has been used to study ${}^3\text{He}(\alpha, \gamma){}^7\text{Be}$ capture processes both for bound and scattering states and has been able to get the resonances for various states with good accuracy.

Zhaba and Laha et al., have shown interest in PFM method. They have studied nucleon nucleon, nucleon-nucleus and nucleus-nucleus interaction [7] [18] using PFM methodology in tandem with supersymmetric quantum mechanics (SUSY-QM) with free running parameters and obtained reasonably good results. They used double Hulthen and Manning-Rosen phenomenological potentials as models of nuclear potentials. We instead in this paper are using well known Morse potential with PFM. Earlier, we have applied PFM for studying np, n-d and $\alpha - \alpha$ system [19, 20] using Morse potential and keeping the binding energy of the system intact we obtained the SPS with good accuracy to that of the experimental data given in literature. In this paper, in addition to the inter-nuclear and Coulomb interactions, we have added a non-local interaction in the form of Spin-Orbit coupling for obtaining the SPS for various J-channels. The ℓ -dependence due to centrifugal potential is already incorporated in the PFM equation and hence does not need to be considered separately. Experimental data has been taken from Hardy et al. [3] (5.69-13.47 MeV) and Bokyin et al. [4] (3.30-6.86 MeV). Spiger et al. [5] measured differential elastic scattering cross section and fitted the experimental phase shift data using R-matrix method. Although Spiger et al. has taken all energies from ≈ 4 -18 MeV which carries double resonance peaks yet the phase analysis is available only in graphical format and not available in tabulated form. Hardy et al., and Bokyin [3, 4] have presented their data in tabulated form and hence these are chosen for SPS computations during this work.

2. Methodology

2.1. Modeling α - ${}^3\text{He}$ using Morse Potential with Spin-orbit Coupling

The interaction is modeled by using Morse potential [21] given by :

$$V_M(r) = V_0 \left(e^{-2(r-r_m)/a_m} - 2e^{-(r-r_m)/a_m} \right) \quad (1)$$

Here V_0 is potential depth, r_m is equilibrium distance where $V = V_0$ and a_m is the shape parameter that suggests the decaying rate with increasing distance. The Coulomb interaction is considered to be of the form [22]. $z_1 \times z_2 = 4$ for interacting particles.

$$\begin{aligned} V_C &= \frac{4e^2}{r} \text{erf}(\beta r) \text{ where } \text{erf}(\beta r) \\ &= \frac{2}{\sqrt{\pi}} \int_0^{\beta r} \exp(-x^2) dx \text{ and } \beta \\ &= \frac{\sqrt{3}}{2R_\alpha} = 0.47 \text{ fm}^{-1} \end{aligned} \quad (2)$$

The parameter β is inversely related to root mean square (RMS) radius of interacting system. We chose root mean square radius $R = 1.826$ fm for α - ${}^3\text{He}$ system. The spin orbit coupling potential is obtained, after differentiating the Morse potential, as

$$V_{LS}(r) = \left(\frac{r_0}{\hbar} \right)^2 \frac{1}{r} \frac{2V_0}{a_m} \left[e^{-(r-r_m)/a_m} - e^{-2(r-r_m)/a_m} \right] (\vec{L}, \vec{S}) \quad (3)$$

Here, $\vec{L}, \vec{S} = \frac{\hbar^2}{2} [J(J+1) - L(L+1) - S(S+1)]$. The proportionality constant r_0^2 takes care of dimensional analysis and also adds an extra parameter for optimization. Finally, the total interaction potential V_T takes the following form with central, Coulomb and spin-orbit incorporated in the total interaction potential

$$\begin{aligned} V_T &= V_0 \left(e^{-2(r-r_m)/a_m} - 2e^{-(r-r_m)/a_m} \right) \\ &+ \left(\frac{r_0}{\hbar} \right)^2 \frac{1}{r} \frac{2V_0}{a_m} \left[e^{-(r-r_m)/a_m} - e^{-2(r-r_m)/a_m} \right] (\vec{L}, \vec{S}) \\ &+ \frac{4e^2}{r} \text{erf}(\beta r) \end{aligned}$$

2.2. Optimization of Model Parameters

The SPS have been determined, using PFM for the Morse function interaction, by fitting the parameters so as to obtain the minimum value for mean absolute percentage error (MAPE)-value, defined as

$$MAPE = \frac{1}{N} \sum_{i=1}^N \frac{|\delta_i^{\text{exp}} - \delta_i^{\text{sim}}|}{|\delta_i^{\text{exp}}|} \times 100 \quad (4)$$

Where δ_i^{exp} and δ_i^{sim} are the experimental and simulated phase shift values at different energies E_i and N is the number of experimental data points considered. This parameter can be considered as one of the good measures to compare two sets of data. The smaller the resulting value of $MAPE$, the better the match between the two data sets.

2.3. Phase Function Method (PFM)

The Schrodinger wave equation for a spinless particle with energy E and orbital angular momentum ℓ undergoing scattering with interaction potential $V(r)$ is given by

$$\frac{\hbar^2}{2\mu} \left[\frac{d^2}{dr^2} + (k^2 - \ell(\ell+1)/r^2) \right] u_\ell(k, r) = V(r) u_\ell(k, r) \quad (5)$$

where $k_{c.m.} = \sqrt{E_{c.m.} / (\hbar^2 / 2\mu)}$. For system ${}^3\text{He}(\alpha, \gamma){}^7\text{Be}$ centre of mass energy $E_{c.m.}$ is related to laboratory energy by following relation for non-relativistic kinematics

$$E_{c.m.} = \frac{M_\alpha}{M_\alpha + M_{\frac{3}{2}\text{He}}} E_{lab.} \approx 0.57 E_{lab.} \quad (6)$$

The value of $\hbar^2 / 2\mu = 12.15 \text{ MeV fm}^2$ for α - ${}^3\text{He}$ system. The mathematical foundation of PFM method is well known in theory of differential equations, that a linear homogeneous equation of second order, such as Schrodinger equation, can be reduced to a nonlinear differential equation (NDE) of first order - the Riccati equation [23]. The phase equation which was independently worked out by Calogero [24] and Babikov [25] is written in the following form.

PFM or variable phase approach (VPA) is one of the important tools in scattering studies for both local [24] and

$$\delta'_3(k, r) = -\frac{V(r)}{k} \left[\frac{(kr)^3 \cos(\delta_3 + kr) - 6(kr)^2 \sin(\delta_3 + kr) - 15kr \cos(\delta_3 + kr) + 15 \sin(\delta_3 + kr)}{(kr)^3} \right]^2 \quad (11)$$

These NDE's equations (9-11) are numerically integrated from origin to the asymptotic region using RK-4/5 method, thereby obtaining directly the values of scattering phase shift for different values of projectile energy in lab frame. The central idea of VPA is to obtain the phase shift $\delta(k, r)$ directly from physical quantities such as interaction potential $V(r)$, instead of solving TISE for wave functions $u(r)$, which in turn are used to determine $\delta(k, r)$.

non-local interactions [26]. The second order differential equation Eq.5 can be transformed to the first order non-homogeneous differential equation of Riccati type [24, 25], given by

$$\delta'_\ell(k, r) = -\frac{V(r)}{k} \left[\cos(\delta_\ell(k, r)) \hat{j}_\ell(kr) - \sin(\delta_\ell(k, r)) \hat{\eta}_\ell(kr) \right]^2 \quad (7)$$

Prime denotes differentiation of phase shift with respect to distance and the Riccati Hankel function of first kind is related to $\hat{j}_\ell(kr)$ and $\hat{\eta}_\ell(kr)$ by $\hat{h}_\ell(r) = -\hat{\eta}_\ell(r) + i \hat{j}_\ell(r)$. In integral form, the above equation can be written as

$$\delta_\ell(k, r) = -\frac{1}{k} \int_0^r V(r) \left[\cos(\delta_\ell(k, r)) \hat{j}_\ell(kr) - \sin(\delta_\ell(k, r)) \hat{\eta}_\ell(kr) \right]^2 dr \quad (8)$$

The function $\delta_\ell(k, r)$ is called the phase function. The advantage of this method is that, the phase-shifts are directly expressed in terms of the potential and have no relation to the wavefunction. Also, rather than solving the second order Schrodinger equation we only need to solve the first order non-homogeneous differential equation of Riccati type, given by Eq.7, for phase shift calculations. For S -partial wave ($\ell = 0$), the Riccati-Bessel and Riccati-Neumann functions \hat{j}_0 and $\hat{\eta}_0$ get simplified as $\sin(kr)$ and $-\cos(kr)$, so the phase equation for $\ell = 0$ takes the form

$$\delta'_0(k, r) = -\frac{V(r)}{k} \sin^2 [kr + \delta_0(k, r)] \quad (9)$$

The phase function equation for $\ell = 1$ i.e. P-partial wave, is of the form

$$\delta'_1(k, r) = -\frac{V(r)}{k} \left[\frac{\sin(\delta_1 + kr) - kr \cos(\delta_1 + kr)}{kr} \right]^2 \quad (10)$$

and PFM equation for F- wave takes following form

3. Results and Discussion

The model parameters for Morse potentials obtained on minimising the MAPE for various ℓ -channels have been tabulated in Table 1. Scattering phase shifts (SPS) are computed upto ≈ 8 MeV which is above proton separation threshold at which excitation function becomes fat in nature [27]. In figure 1(a) and 1(b), the obtained SPS for

$\delta^{7/2^-}$, $\delta^{5/2^-}$, $\delta^{1/2^-}$, $\delta^{3/2^-}$ and $\delta^{1/2^+}$ channels are shown. These SPS are in good match with experimental data of Boykin *et al.* [4] with MAPE for all the states given in Table 1. In figure 1(a), solid black color represents the F7/2⁻ phase shift. While S-wave, i.e., S1/2⁺, is dominating at low energies, F7/2⁻ and F5/2⁻ are negligible at low energies. Their SPS starts to become visible at E>4 MeV. F-wave contribution is negligibly small at energies $E_{lab} = 0-4$ MeV, after which it has sharp jump to 1800 in SPS for

Table 1: ${}^3\text{He}(\alpha,\gamma){}^7\text{Be}$ scattering phase shifts parameters with erroneous data removed.

State	V_0 (MeV)	r_m (fm)	a_m (fm)	r_0	MAPE(%)
1/2 ⁺	2.1028	4.5952	2.0439	-	3.2
1/2 ⁻	13.4386	3.0030	1.6853	0.1428	1.0
3/2 ⁻	14.3404	2.9040	1.6191	0.2014	0.81
5/2 ⁻	38.7823	0.0064	1.2136	1.1922	17.6
7/2 ⁻	166.6467	0.4206	0.8621	0.1161	6.5

Table 2: Computed ${}^3\text{He}(\alpha,\gamma){}^7\text{Be}$ scattering phase shifts for 1/2⁺, 1/2⁻, 3/2⁻, 5/2⁻ and 7/2⁻ states upto 7.95 MeV for laboratory energies obtained using Morse potential model along side those of experimental ones [3, 4]. Bottom row shows MAPE value. Energies having erroneous phase shift (energies shown in bold) values are not taken during calculations.

E_{lab} . (MeV)	1/2 ⁺	SIM.	1/2	SIM.	3/2	SIM.	5/2	SIM.	7/2	SIM.
3.30	-23±2	-21.153	162±3	162	165±1	165.234	0±1	-	2±1	1.276
3.51	-24±1	-23.304	161±1	161.014	164±1	164.000	2±1	1.242	2±1	1.733
3.88	-27±1	-27.000	159±2	158.81	162±1	161.721	2±1	1.788	3±1	2.999
4.37	-30±1	-31.674	156±2	155.207	158±1	158.534	3±1	2.783	7±1	6.683
4.46	-31±1	-	156±2	-	158±1	-	5 ±1	-	7±1	-
4.64	-33±2	-34.129	153±2	153	158±1	156.714	5 ±1	3.499	10±1	11.449
4.79	-34±1	-35.455	151±2	151.729	157±2	155.688	5 ±1	3.958	15±1	16.47
4.95	-40±6	-	150±3	-	154±2	-	3 ±1	-	23±4	-
5.09	-49±7	-	146±5	-	153±3	-	4±2	-	40±4	-
5.21	-38±5	-39.014	149±3	148.065	153±2	152.775	3±1	5.53	78±4	77.979
5.69	-45.9	-42.805	132.6	-	149.4	149.4	8	7.987	157.4	153.335
6.04	-50±7	-	137±5	-	142	-	11±4	-	165±3	-
6.19	-47.7	-46.442	134.9	139.425	141.9	145.873	10.6	11.608	166.2	163.347
6.45	-50.3	-48.211	133.9	137.202	140.9	144.045	11.9	14.082	167.6	165.278
6.46	-49±5	-	139±3	-	140±2	-	15±3	-	169±2	-
6.86	-48±9	-	139±4	-	140±4	-	17±4	-	174±3	-
6.95	-54.1	-51.384	131	133.076	137.5	140.563	18.6	20.456	169.6	167.187
7.20	-52.0	-52.863	131.1	131.1	136.5	138.843	23.9	24.7	170.9	167.703
7.70	-56.5	-55.618	130	127.338	135.5	135.463	36.1	36.096	171	168.305
7.95	-56.9	-56.9	127.9	125.556	133.8	133.8	46.7	43.532	172	168.471
MAPE		3.2		1.0		0.81		17.6		6.5

7/2⁻, which can be observed to be responsible for its potential have a strong attractive character as in figure (a). On the other hand, SPS for 5/2⁻ are seen to be increasing slowly as compared to 7/2⁻ and hence the corresponding potential is less attractive in comparison. SPS for P1/2⁻, S1/2⁺ and P3/2⁻ are shown in figure 1(b). One can observe

that S1/2⁺ SPS are in good fit with respect to experimental data [3, 4]. It should be noted that for E< 3 MeV, the computed values are extrapolated and are found to touch at 0°. Similarly, SPS for 1/2⁻ and 3/2⁻ of P-waves, are also found to be in good match with the experimental data with MAPE of 1.0% and 0.81% respectively. For SPS at lower

energies, where no experimental data is available, the SPS are extrapolated and found to touch at 180° at 0 MeV. Those of $3/2^-$ have been shifted such that the extrapolated data towards lower energies are seen to reach 90° . To conclude, sharp jump in phase shifts is an indication of resonance with sharply varying potential curves.

Ground state for ${}^7\text{Be}$ is $3/2^-$ while $1/2^-$ state is just above it with experimental energies of -1.587 MeV and -1.157 MeV respectively [12]. Our potentials follows the same trend with $3/2^-$ state potential just below $1/2^-$ state. Table 2 shows computed ${}^3\text{He}(\alpha,\gamma){}^7\text{Be}$ scattering phase shifts for various states upto 7.95 MeV laboratory energies. Data shown in bold is removed from the computations so that least errors in phase shifts could provide better trend for computations at higher energies.

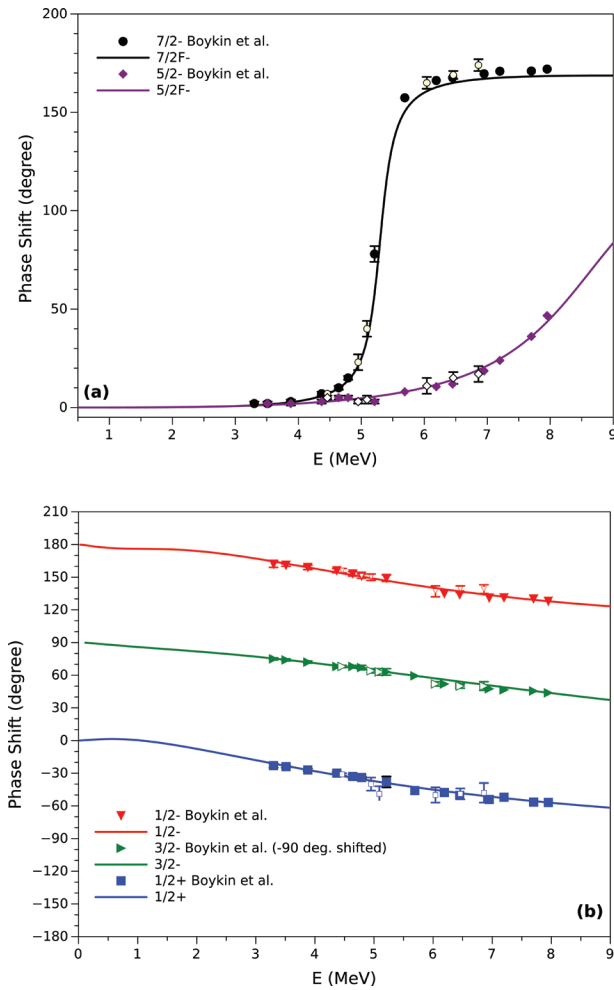


Figure 1: ${}^3\text{He}-\alpha$ scattering phase shifts for (a) resonant states $\delta^{7/2^-}$ and $\delta^{5/2^-}$ state and (b) resonant states $\delta^{1/2^-}$, $\delta^{3/2^-}$ and non resonant state $\delta^{1/2^+}$ channels as a function of laboratory energy. Data shown without any filled colour contains maximum error in phase shift and is ignored during computations.

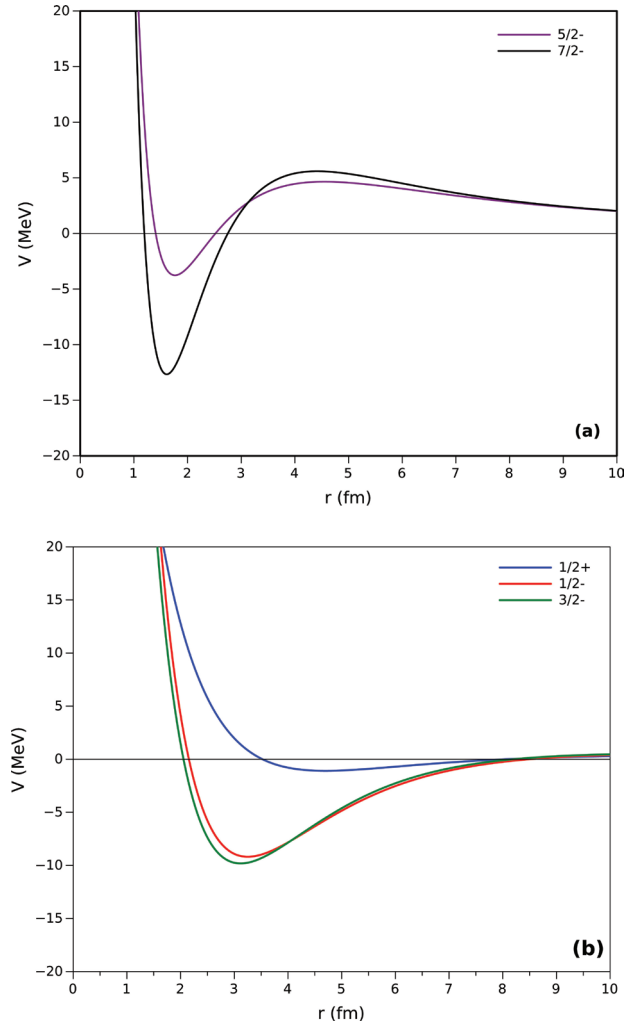


Figure 2: Total potentials are portrayed (a) shows $5/2^-$ and $7/2^-$ state potentials while (b) shows $1/2^+$, $1/2^-$ and $3/2^-$ state potentials.

3.1. Cross Section

Partial cross section is shown in figure 3 for different states calculated using the obtained phase shift values.

Partial cross section has been calculated by expression:

$$\sigma_\ell = \frac{4\pi}{k^2} (2\ell + 1) \sin^2 \delta_\ell(k) \quad (12)$$

while the total cross section is given by [28]

$$\sigma_T = \frac{4\pi}{k^2} \sum_\ell \{ (\ell + 1) \sin^2 \delta_\ell^+ + \ell \sin^2 \delta_\ell^- \} \quad (13)$$

In above equation δ^\pm indicates scattering phase shifts for $J = \ell \pm 1/2$ states, where $\ell \geq 1$. We have computed scattering phase shifts upto ≈ 8 MeV which is above proton separation threshold at which excitation function

becomes flat in nature [27]. This region (0-8 MeV) takes care of $7/2^-$ first resonance while leaves the first resonance for $5/2^-$ state. In figure 3 we have shown first resonance peak for $5/2^-$ state by considering phase shift data upto ≈ 13 MeV for V_0 , r_m , a_m and r_0 is 41.8165, 0.8941, 1.0052 and 0.7599 respectively. For $7/2^-$ first resonance energy is computed to be 3.02 MeV while experimental value is 2.98 MeV.

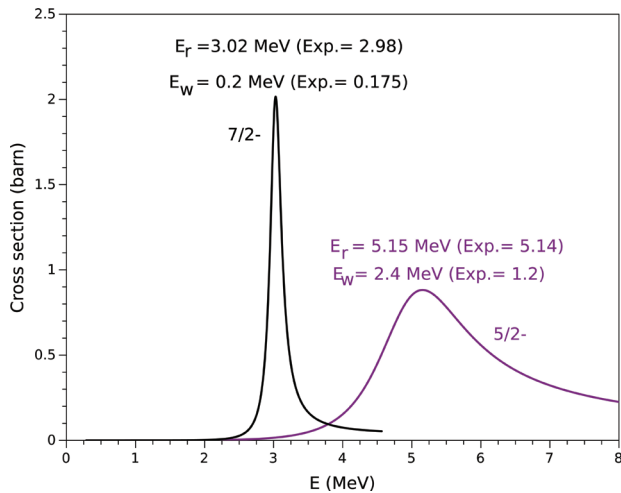


Figure 3: ${}^3\text{He}$ - α cross section for resonant states and width respectively in centre of mass $E_{c.m.}$.

Resonance width Γ for the same state is 0.2 MeV, while experimental value is 0.175 MeV. Thus our simulated resonance energy and resonance width is close to the experimental values [12]. Here it is to be noted that sharp change in phase shift with energy give important contribution to cross section which we observe as resonating peaks with deep attractive potential. For $5/2^-$ resonance $E_R=5.15$ MeV while experimental value is 5.14 [12] MeV, while computed resonance width Γ is 2.4 which is found to be twice to the experimental value of 1.2 MeV, because $5/2^-$ is a broad state.

It would be interesting to see how this Morse potential will fare in explaining other important astrophysical reactions. Moreover, new experimental studies, especially for $3/2^+$ and $5/2^+$ states, would be highly desired of the α - ${}^3\text{He}$ elastic scattering, as no recent experimental data is available in past 50 years or so, to probe more accurately the quality of the scattering phase shifts and obtain structure information.

Conclusion

Scattering phase shifts are the key outputs of any nuclear reaction. It provides the knowledge of the interaction between the interacting particles. Here we have computed the interaction potentials for different ${}^7\text{Be}$ states by

using the phase shift data. Phase function method tied with suitable optimisation technique helps to obtain the interaction potential. Using Morse potential as model of interaction and its derivative as spin-orbit term, the parameters are optimised to minimise mean absolute percentage error between the simulated scattering phase shifts obtained using phase function method and experimental values. The MAPEs for various ℓ -channels $1/2^+$, $1/2^-$, $3/2^-$, $5/2^-$ and $7/2^-$ states upto 7.95 MeV for laboratory energies to be 3.2, 1.0, 0.81, 17.6 and 6.5 respectively. The partial cross sections for $7/2^-$ and $5/2^-$ states of ${}^3\text{He}(\alpha, \gamma){}^7\text{Be}$ reaction have been determined and their respective resonance energies are found to be 3.02 ± 0.2 MeV and 5.15 ± 2.4 MeV. All these calculations can help to calculate astrophysical S-factor of any thermonuclear reaction i.e. $S(E)$ for lower energies, which will be our future goal.

Acknowledgements

We would like to thank the anonymous reviewers for their suggestions and comments for further improvement of the paper.

Authorship contribution

Anil Khachi & Lalit Kumar: Data curation; formal analysis; investigation; methodology; resources; software; validation; visualization; writing-original draft.

OSKS Sastri: Conceptualization; formal analysis; investigation; methodology; project administration; resources; software; supervision; validation; visualization; writing-review editing.

Funding

We hereby state that there is no funding received for this work.

Conflict of interest

There is no conflict of interest whatsoever.

Declaration

It is an original data and has neither been sent elsewhere nor published anywhere.

References

- [1] E. Adelberger et al., Rev. Mod. Phys. **83**, 195 (2011). <https://doi.org/10.1103/RevModPhys.83.195>
- [2] P. D. Serpico et al., JCAP **12**, 10 (2004). <https://doi.org/10.1088/1475-7516/2004/12/0100>

- [3] D. M. Hardy, R.W.J. Spiger and S.D. Baker, Nucl. Phys. A **195**, 241 (1972).
[https://doi.org/10.1016/0375-9474\(72\)90733-6](https://doi.org/10.1016/0375-9474(72)90733-6)
- [4] W. R. Boykin, S. D. Baker and D. M. Hardy, Nucl. Phys. A **195**, 241 (1972).
[https://doi.org/10.1016/0375-9474\(72\)90732-4](https://doi.org/10.1016/0375-9474(72)90732-4)
- [5] R. J. Spiger, T. A. Tombrello, Phys. Rev. C **163**, 964 (1967). <https://doi.org/10.1103/PhysRev.163.964>
- [6] J. D. Eraly, Phys. Lett. B **757**, 430 (2016).
<https://doi.org/10.1016/j.physletb.2016.04.021>
- [7] J. Bhoi and U. Laha, Phys. At. Nucl. **79**, 370 (2016).
<https://doi.org/10.1134/S1063778816030054>
- [8] A. V. Dobrovolsky et al., Nucl. Phys. A **989**, 40 (2019).
<https://doi.org/10.1016/j.nuclphysa.2019.05.012>
- [9] S. B. Doubovichenko, A. V. Dzhezairov-Kakhramanov, Phys. Atom. Nucl. **58**, 579 (1995).
arXiv:nucl-th/9802080
- [10] R. Christy and I. Duck, Nucl. Phys. **24**, 89 (1961).
[https://doi.org/10.1016/0029-5582\(61\)91019-7](https://doi.org/10.1016/0029-5582(61)91019-7)
- [11] W. C. Haxton, R. G. Hamish Robertson, and A. M. Serenelli, Ann. Rev. Astron. **51**, 21 (2013).
<https://doi.org/10.1146/annurev-astro-081811-125539>
- [12] D. R. Tilley et al., Nucl. Phys. A **708**, 3 (2002).
[https://doi.org/10.1016/S0375-9474\(02\)00597-3](https://doi.org/10.1016/S0375-9474(02)00597-3)
- [13] H. W. Hammer, C. Ji, and D. R. Phillips, J. Phys. G **44**, 103002 (2017).
<https://doi.org/10.1088/1361-6471/aa83db>
- [14] T. Kajino, H. Toki, and S. M. Austin, Astrophys. J. **319**, 531 (1987).
- [15] K. M. Nollett and S. Burles, Phys. Rev. D **61**, 123505 (2000).
<https://doi.org/10.1103/PhysRevD.61.123505>
- [16] R. S. Mackintosh, arXiv preprint arXiv:1205.0468 (2012).
- [17] R. Jost and A. Pais, Phys. Review **82**, 840 (1951).
<https://doi.org/10.1103/PhysRev.82.840>
- [18] V. I. Zhaba, International Journal of Modern Physics E **25**, 1650088 (2016).
<https://doi.org/10.1142/S0218301316500889>
- [19] A. Khachi, L. Kumar and O. S. K. S Sastri, J. Nucl. Phys. Mat. Sci. Rad. A **9**, 87 (2021).
<https://doi.org/10.15415/jnp.2021.91015>
- [20] A. Khachi, L. Kumar, A. Sharma and O. S. K. S Sastri, J. Nucl. Phys. Mat. Sci. Rad. A **9**, 1 (2021).
<https://doi.org/10.15415/jnp.2021.91001>
- [21] P. M. Morse, Phys. Rev. **34**, 57, (1929).
<https://doi.org/10.1103/PhysRev.34.57>
- [22] S. Ali and A. R. Bodmer, Nuclear Physics **80**, 99 (1966).
[https://doi.org/10.1016/0029-5582\(66\)90829-7](https://doi.org/10.1016/0029-5582(66)90829-7)
- [23] G. N. Watson, Theory of Bessel Functions (Cambridge University Press, 1945).
- [24] F. Calogero, American Journal of Physics **36**, 566 (1968). <https://doi.org/10.1119/1.1975005>
- [25] V. V. Babikov, SOV PHYS USPEKHI **10**, 271 (1967).
<https://doi.org/10.1070/PU1967v010n03ABEH003246>
- [26] B. Talukdar, D. Chatterjee, and P. Banerjee, J. Phys. G, Nucl. Phys. **3**, 813 (1977).
- [27] T. Szucs, G. Gyurky, Z. Halasz, G. G. Kiss and Z. Fulop, In EPJ Web of Conferences **165** 01049 (2017).
<https://doi.org/10.1051/epjconf/201716501049>
- [28] P. E. Hodgson, Adv. Phys., **25**, 1 (1958).
<https://doi.org/10.1080/00018735800101157>



Journal of Nuclear Physics, Material Sciences, Radiation and Applications

Chitkara University, Saraswati Kendra, SCO 160-161, Sector 9-C, Chandigarh, 160009, India

Volume 9, Issue 2

February 2022

ISSN 2321-8649

Copyright: [© 2022 Anil Khachi, Lalit Kumar and O.S.K.S. Sastri] This is an Open Access article published in Journal of Nuclear Physics, Material Sciences, Radiation and Applications (J. Nucl. Phys. Mat. Sci. Rad. A.) by Chitkara University Publications. It is published with a Creative Commons Attribution- CC-BY 4.0 International License. This license permits unrestricted use, distribution, and reproduction in any medium, provided the original author and source are credited.